



UNIVERSITI PUTRA MALAYSIA

***SYNTHESIS AND CHARACTERIZATION OF TRANSPARENT
SUPERHYDROPHOBIC FLUORINATED GRAPHENE OXIDE
AND SILICA BASED SOL GEL COATING FILMS***

MOHD HAMZAH BIN HARUN

FS 2020 44



**SYNTHESIS AND CHARACTERIZATION OF TRANSPARENT
SUPERHYDROPHOBIC FLUORINATED GRAPHENE OXIDE
AND SILICA BASED SOL GEL COATING FILMS**

By

MOHD HAMZAH BIN HARUN

**Thesis Submitted to the School of Graduate Studies, Universiti
Putra Malaysia, in Fulfilment of the Requirements for the Degree of
Doctor of Philosophy**

September 2020

All material contained within the thesis, including without limitation text, logos, icons, photographs and all other artwork, is copyright material of Universiti Putra Malaysia unless otherwise stated. Use may be made of any material contained within the thesis for non-commercial purposes from the copyright holder. Commercial use of material may only be made with the express, prior, written permission of Universiti Putra Malaysia.

Copyright © Universiti Putra Malaysia



DEDICATION

To my parents, Hajah Zarah binti Taib, Haji Harun bin Abdul Ghani, my wife, Dr. Norfazlinayati Othman, my lovely children, family, in-laws, supervisors and the lecturers, colleagues, relatives, friends and who have given me all supports, loves and patience.

Thank you very much.



Abstract of the thesis presented to the Senate of Universiti Putra Malaysia in fulfillment of the requirement for the degree of Doctor of Philosophy

**SYNTHESIS AND CHARACTERIZATION OF TRANSPARENT
SUPERHYDROPHOBIC FLUORINATED GRAPHENE OXIDE
AND SILICA BASED SOL GEL COATING FILMS**

By

MOHD HAMZAH BIN HARUN

September 2020

Chairperson : Professor Zainal Abidin Talib, PhD
Faculty : Science

Transparent water repellent organosilica based coating containing tetraorthosilicate (precursor), fluoroalkylsilane (hydrophobic agent) and nanofillers (roughness agent) were prepared by sol-gel method. The coating was prepared by modification of silica (SiO_2) or graphene oxide (GO) nanofillers with siloxane having long chain fluoroalkylsilane that allow for reducing surface energy. Four different samples were prepared namely, tetraorthosilicate sol (TEOS sol), tetraorthosilicate-fluoroalkylsilane (TEOS-FAS), tetraorthosilicate-fluoroalkylsilane-silica (TEOS-FAS- SiO_2) and tetraorthosilicate-fluoroalkylsilane-graphene oxide (TEOS-FAS-GO). The hydrophobic coating solutions were prepared at different concentration percentages of silica and GO ranging from 0.04 pph - 0.20 pph respectively. The water contact angle, transmittance degree, surface morphology and topography, chemical composition and surface analysis were characterized by Attension Tensiometer, UV-Visible Spectrophotometer, Field Emission Scanning Electron Microscope (FESEM), Atomic Force Microscope (AFM), Fourier Transform Infrared Spectroscopy (FTIR), and X-Ray Photoelectron Spectroscopy (XPS).

The contact angle for TEOS sol formulation at different concentrations of tetraorthosilicate showed a hydrophilic behavior in which the contact angle measured was lower than 90° whereas for TEOS-FAS formulation, hydrophobic behavior was obtained in which the measured contact angles were between 90° and 115° . For TEOS-FAS- SiO_2 and TEOS-FAS-GO, the contact angles obtained were in the range of pre-superhydrophobic and superhydrophobic range (120° - 168°). Such behavior can be explained by the presence of hydrophobic agents which were fluoroalkylsilane and nanosize fillers which were SiO_2 and GO. To

investigate the durability of hydrophobicity value, the contact angle after peeling test using Scotch tape was measured. It showed that the TEOS-FAS-GO is more durable as the drop of contact angle value is more gradual as compared with other samples.

The transmittance for all samples showed that they were transparent and the range obtained was between 70% - 95%. FESEM images confirmed the presence of silica and GO in the samples in which for TEOS-FAS-SiO₂, uniform structure was obtained whereas for TEOS-FAS-GO, it showed that the silica from TEOS grew onto the graphene flakes. FTIR showed that the most important peak at 1036-1055 cm⁻¹ has been obtained which confirmed the covalent attachment of FAS with silanol particles within tetraorthosilicate matrix in TEOS-FAS-GO and TEOS-FAS-SiO₂ formulation. AFM demonstrated that the roughness increased with the addition of silica and GO fillers with TEOS-FAS-GO gave relatively greater roughness than TEOS-FAS-SiO₂ samples. XPS analysis showed that FAS and TEOS molecules were successfully grafted on the SiO₂ and GO surfaces with hydroxyl and carboxyl groups were involved as well as silica nanoparticles from TEOS sol for TEOS-FAS-GO and silica nanoparticles itself for TEOS-FAS-SiO₂.

The introduction of SiO₂ and GO in the formulation of transparent TEOS sol formulation containing long chain fluoroalkylsilane enhance the surface roughness and thus induces the hydrophobicity in which the water contact angle obtained in the range of hydrophobicity and superhydrophobicity (120° - 169°). This indicates that the surface roughness plays an important role in enhancing hydrophobicity and lowering the surface free energy. Although the transmittance degrees obtained were slightly lower than TEOS sol and TEOS-FAS formulation which were around 70-95%, the transmittance is still within the accepted level since the hydrophobic coatings obtained were visible.

Abstrak tesis ini dikemukakan kepada Senat Universiti Putra Malaysia sebagai memenuhi keperluan untuk penganugerahan ijazah Doktor Falsafah

**SINTESIS DAN PENCIRIAN FILEM SALUTAN SUPERHIDROFOBIA
LUTSINAR SOL GEL BERASASKAN SILIKA DAN
GRAFIN OKSIDA TERFLUORIN**

Oleh

MOHD HAMZAH BIN HARUN

September 2020

Pengerusi : Profesor Zainal Abidin Talib, PhD
Fakulti : Sains

Salutan kalis air lutsinar berasaskan organosilika yang mengandungi tetraorthosilikat (prekursor), fluoroalkilsilana (agen hidrofobik) dan pengisi nano (agen kekasaran) telah disediakan menggunakan kaedah sol-gel. Salutan tersebut telah disediakan dengan modifikasi pengisi nano silika atau grafin dengan siloksana yang mempunyai rantai panjang fluoroalkilsilana yang membolehkan ia menurunkan tenaga permukaan. Empat sampel berbeza telah disediakan iaitu sol tetraorthosilikat (sol TEOS), sol tetraorthosilikat fluoroalkilsilana (TEOS-FAS), tetraorthosilikat-fluoroalkilsilana-silika (TEOS-FAS-SiO₂) dan tetraorthosilikat fluoroalkilsilana-grafin oksida (TEOS-FAS-GO). Larutan salutan hidrofobik telah disediakan pada purata kepekatan berbeza iaitu dari 0.04 pph hingga 0.20. Sudut sentuh air, darjah kepancaran, morfologi dan topografi permukaan, komposisi kimia dan analisa permukaan dicirikan dengan alat Attension Tensiometer, Meter Spektro UV-Tampak, Mikroskop Elektron Imbasan Medan Pancaran (FESEM), Mikroskop Daya Atom (AFM) Infra-Merah Transformasi Fourier (FTIR) dan Spektroskopi X-Ray.

Sudut sentuh untuk formulasi sol TEOS pada kepekatan berbeza tetraorthosilikat menunjukkan yang ia mempunyai sifat hidrofilik yang mana sudut sentuh yang diukur adalah lebih rendah daripada 90° berbanding dengan formulasi TEOS-FAS, sifat hidrofobik diperoleh dengan sudut sentuh diukur adalah di antara 90° dan 115°. Sudut sentuh yang berbeza diperoleh bagi TEOS-FAS-SiO₂ dan TEOS-FAS-GO yang mana sudut sentuh diperolehnya dalam julat prasuperhidrofobik dan superhidrofobik (120° - 168°). Sifat sebegini boleh dijelaskan dengan kehadiran agen hidrofobik iaitu fluoroalkilsilana dan pengisi bersaiz nano iaitu SiO₂ and GO. Untuk menyiasat ketahanan nilai hidrofobik, sudut sentuh selepas ujian kupasan menggunakan pita Scotch telah diukur. Ia menunjukkan yang TEOS-FAS-GO lebih tahan memandangkan penurunan nilai

sudut sentuh lebih seragam berbanding sampel-sampel lain. Darjah transmisi untuk kesemua sampel menunjukkan yang setiap darinya lut sinar dan julat diperoleh ialah 70% - 95%. Imej FESEM mengesahkan kehadiran silika dan GO pada sampel yang mana struktur uniform bagi TEOS-FAS-SiO₂ didapati manakala bagi TEOS-FAS-GO, ia menunjukkan silika yang terhasil daripada TEOS tumbuh pada empingan grafin. FTIR menunjukkan yang puncak penting adalah pada 1036-1055 cm⁻¹ s yang mengesahkan berlakunya sangkutan kovalen oleh FAS terhadap partikel silanol dalam matriks tetraorthosilikat bagi formulasi TEOS-FAS-GO dan TEOS-FAS-SiO₂. AFM menunjukkan yang kekasaran meningkat dengan penambahan pengisi silika dan GO dan TEOS-FAS-GO memberikan nilai kekasaran yang sangat tinggi. Analisis XPS menunjukkan molekul TEOS dan FAS terancang pada permukaan SiO₂ dan GO dengan kumpulan berfungsi hidroksil dan karboksil terlibat dan juga partikel nano silika daripada sol TEOS untuk TEOS-FAS-GO dan partikel nano silika unuk TEOS-FAS-SiO₂.

Penampilan SiO₂ dan GO dalam formulasi sol TEOS lutsinar yang mengandungi fluoroalkilsilana rantai panjang meningkatkan kekasaran permukaan dan tahap hidrofobik di mana sudut sentuh air diperoleh dalam julat hidrofobik dan superhidrofobik. Ini menunjukkan yang kekasaran permukaan memainkan peranan penting dalam meningkatkan tahap hidrofobik dan menurunkan tenaga permukaan bebas. Walaupun darjah transmisi yang didapati sedikit rendah bagi TEOS-FAS-SiO₂ dan TEOS-FAS-GO daripada formulasi sol TEOS dan TEOS-FAS iaitu sekitar 70-95%, transmisi diperoleh masih pada tahap boleh diterima memandangkan salutan hidrofobik yang didapati adalah boleh tampak.

ACKNOWLEDGEMENT

In the name of Allah, the most Gracious and the most Merciful.

Praise is to Allah the Almighty, for thee (alone) we worship and thee (alone) we ask for help. Praise also is upon Muhammad S.A.W. who is guidance and has led us to the path that God has favored.

First of all, I would like to express my gratitude to my parents Haji Harun Abdul Ghani and Hajah Zarah Taib, my lovely wife, Dr. Fazlina and my children Hasanah, Nasrul and Hidayat, families and in-laws for their patience, support, courage and understanding. Secondly, my acknowledgement goes to my supervisor, Professor Dr. Zainal Abidin Talib for keeping his confidence to see me complete my PhD. program and all the patience, advice, constructive comments, encouragement, in helping me to finish my postgraduate study, my deepest gratitude goes to you. I also would like to express my appreciation to my co-supervisors, namely Associate Prof. Dr. Nor Azowa Ibrahim and to Dr. Josephine Liew Ying Chyi for their moral support, technical discussion as well as contribution. I would also like to express my gratitude to Dr. Nik Ghazali Nik Salleh, my former manager in Malaysian Nuclear Agency who has groomed and nurtured me to become where I am now. Thanks to all of you.

Not to forget to my research fellows in Malaysian Nuclear Agency, to name a few, Mr. Mohd Sofian Alias, Mr. Mahathir Mohamed and the rest of RadCure group, Radiation Processing Technology Division (BTS) and MTEG team. Also, to my research colleagues in the Physics Department, to name a few, Dr. Nordin Sabli, Dr Ibrahim, Dr. Joe, Mr. Radzi, Dr. Battoo and Dr. Emma for their help, cooperativeness and support. I also dedicate this appreciation to my office fellows and superiors in Radiation Processing Technology Division and to Malaysian Nuclear Agency for their priceless understanding and facilities that have been provided. Finally, financial support from UPM RUGS Grant (Vote No. 9449900) is greatly acknowledged.

This thesis was submitted to the Senate of Universiti Putra Malaysia and has been accepted as fulfilment of the requirement for the degree of Doctor of Philosophy. The members of the Supervisory Committee were as follows:

Zainal Abidin Talib, PhD

Professor
Faculty of Science
Universiti Putra Malaysia
(Chairman)

Nor Azowa binti Ibrahim, PhD

Associate Professor
Faculty of Science
Universiti Putra Malaysia
(Member)

Josephine Liew Ying Chyi, PhD

Senior Lecturer
Faculty of Science
Universiti Putra Malaysia
(Member)

ZALILAH MOHD SHARIFF, PhD

Professor and Dean
School of Graduate Studies
Universiti Putra Malaysia

Date: 10 December 2020

Declaration by graduate student

I hereby confirm that:

- this thesis is my original work;
- quotations, illustrations and citations have been duly referenced;
- this thesis has not been submitted previously or concurrently for any other degree at any other institutions;
- intellectual property from the thesis and copyright of thesis are fully-owned by Universiti Putra Malaysia, as according to the Universiti Putra Malaysia (Research) Rules 2012;
- written permission must be obtained from supervisor and the office of Deputy Vice-Chancellor (Research and Innovation) before thesis is published (in the form of written, printed or in electronic form) including books, journals, modules, proceedings, popular writings, seminar papers, manuscripts, posters, reports, lecture notes, learning modules or any other materials as stated in the Universiti Putra Malaysia (Research) Rules 2012;
- there is no plagiarism or data falsification/fabrication in the thesis, and scholarly integrity is upheld as according to the Universiti Putra Malaysia (Graduate Studies) Rules 2003 (Revision 2012-2013) and the Universiti Putra Malaysia (Research) Rules 2012. The thesis has undergone plagiarism detection software.

Signature: _____ Date: _____

Name and Matric No.: Mohd Hamzah Bin Harun (GS34423)

Declaration by Members of Supervisory Committee

This is to confirm that:

- the research conducted and the writing of this thesis was under our supervision;
- supervision responsibilities as stated in the Universiti Putra Malaysia (Graduate Studies) Rules 2003 (Revision 2012-2013) are adhered to.

Signature: _____

Name of
Chairman of
Supervisory
Committee:

Prof. Dr. Zainal Abidin Talib

Signature: _____

Name of
Member of
Supervisory
Committee:

Associate Prof. Dr. Nor Azowa Ibrahim

Signature: _____

Name of
Member of
Supervisory
Committee:

Dr. Josephine Liew Ying Chyi

TABLE OF CONTENTS

	Page
ABSTRACT	i
ABSTRAK	iii
ACKNOWLEDGEMENTS	v
APPROVAL	vi
DECLARATION	viii
LIST OF TABLES	xiii
LIST OF FIGURES	xv
LIST OF ABBREVIATIONS	xix
CHAPTER	
1	
INTRODUCTION	
1.1 Overview of Transparent Water Repellent Coating	1
1.2 Problem Statement	3
1.3 Scope of Study	4
1.4 Objectives of the Study	4
1.5 Significances of Study	5
1.6 Thesis Outlines	5
2	
LITERATURE REVIEW	
2.1 Overview of Super/hydrophobicity	7
2.2 Theoretical background of superhydrophobicity	7
2.2.1 Young's mode	7
2.2.2 Wenzel's Mode	9
2.2.3 Cassie & Baxter Mode	10
2.2.4 Transition between Cassie & Baxter and Wenzel mode	10
2.2.5 Surface Free Energy	11
2.2.6 Surface roughness vs. Transparency	15
2.3 Materials for Preparing Transparent Superhydrophobicity	16
2.3.1 Inorganic materials	17
2.3.1.1 Titanium dioxide TiO ₂	17
2.3.1.2 Zinc oxide, ZnO	18
2.3.1.3 Other oxide materials	19
2.3.2 Organic materials	20
2.3.2.1 Carbon based materials	20
2.3.2.2 Polymer based materials	21
2.3.3 Inorganic-organic hybrid materials	22
2.3.4 Silica and Graphene oxide based materials	23
2.3.4.1 Silica	23
2.3.4.2 Graphene oxide	24
2.4 Summary	25

3	METHODOLOGY	
	3.1 Materials	27
	3.2 Pre-treatment of glass substrate	27
	3.3 Preparation of transparent hydrophobic coating	27
	3.3.1 TEOS sol formulation	28
	3.3.2 TEOS-FAS formulation	29
	3.3.3 TEOS-FAS-Silica formulation	30
	3.3.4 TEOS-FAS-GO formulation	33
	3.3.5 Spray Coating of Sol Gel Formulation	33
	3.4 Characterization	35
	3.4.1 X-Ray Photoelectron Spectroscopy (XPS)	35
	3.4.2 Fourier Transform Infrared (FTIR) Spectroscopy	36
	3.4.3 UV-Visible (UV-Vis) Spectroscopy	36
	3.4.4 Thermogravimetric analysis	36
	3.4.5 Field Emission Scanning Electron Microscopy (FESEM)	37
	3.4.6 Atomic Force Microscopy (AFM)	37
	3.4.7 Water Contact Angle Analysis	38
	3.4.8 Surface Profilometry	40
4	RESULTS AND DISCUSSION	
	4.1 X-Ray Photoelectron Spectroscopy (XPS) Studies	41
	4.1.1 XPS wide scan	41
	4.1.1.1 Wide scan spectrum for TEOS sol and TEOS-FAS	41
	4.1.1.2 Wide scan spectrum for silica and GO sol gel films	42
	4.1.2 XPS narrow scan	44
	4.1.2.1 Deconvoluted Si2p spectra	44
	4.1.2.2 Deconvoluted O1s spectra	48
	4.1.2.3 Deconvoluted C1s spectra	53
	4.1.2.4 Deconvoluted F1s spectra	56
	4.2 FTIR Studies	60
	4.2.1 Bare Glass and TEOS sol	60
	4.2.2 TEOS-FAS	64
	4.2.3 TEOS-FAS-SiO ₂	67
	4.2.4 TEOS-FAS-GO	71
	4.3 Transparency Studies by UV-Vis	74
	4.3.1 TEOS sol	74
	4.3.2 TEOS-FAS	75
	4.3.3 TEOS-FAS-SiO ₂	77
	4.3.4 TEOS-FAS-GO	78
	4.4 FE-SEM Studies	79
	4.4.1 TEOS sol and TEOS-FAS	79
	4.4.2 TEOS-FAS-SiO ₂	82
	4.4.3 TEOS-FAS-GO	84
	4.5 AFM Studies	86
	4.5.1 TEOS sol and TEOS-FAS	86
	4.5.2 TEOS-FAS-SiO ₂	87

4.5.3	TEOS-FAS-GO	88
4.6	Thermogravimetric Analysis	90
4.6.1	TEOS sol	90
4.6.2	TEOS-FAS	92
4.6.3	TEOS-FAS-SiO ₂	94
4.6.4	TEOS-FAS-GO	96
4.7	Contact Angle and Surface Free Energy Studies	99
4.7.1	WCA and SFE Studies	99
4.7.1.1	TEOS sol	99
4.7.1.2	TEOS-FAS	101
4.7.1.3	TEOS-FAS-SiO ₂	103
4.7.1.4	TEOS-FAS-GO	106
4.7.2	Contact angle after peeling test	108
5	CONCLUSION AND THE WAY FORWARD	
5.1	Conclusion	112
5.2	The Way Forward	115
	REFERENCES	116
	BIODATA OF STUDENT	130
	LIST OF PUBLICATIONS	131

LIST OF TABLES

Table		Page
2.1	A summary of different materials and methods used in synthesizing superhydrophobic coatings	26
3.1	Formulation with different chemical compositions	28
4.1	Percentage of elements presented in the sol gel film	43
4.2	Results obtained from the deconvolution of XPS spectra for Si2p signal	48
4.3	Results obtained from the deconvolution of XPS spectra for O1s signal	52
4.4	Results obtained from the deconvolution of XPS spectra for C1s signal	56
4.5	Results obtained from the deconvolution of XPS spectra for F1s signal	59
4.6	FTIR absorption bands of bare glass	61
4.7	FTIR absorption bands of TEOS Sol	64
4.8	FTIR absorption bands of TEOS-FAS	67
4.9	FTIR absorption bands of TEOS-FAS-SiO ₂	70
4.10	FTIR absorption bands of TEOS-FAS-GO	71
4.11	Degree of transmittance for TEOS sol coatings	75
4.12	Degree of transmittance for TEOS-FAS sol coatings	76
4.13	Degree of transmittance for TEOS-FAS-SiO ₂ sol coatings	78
4.14	Degree of transmittance for TEOS-FAS-GO sol coatings	79
4.15	Elemental quantitative data analysis represents TEOS and TEOS-FAS coated on the glass microslide	82
4.16	Elemental quantitative data analysis represents TEOS-FAS-Silica coated on the glass microslide	84

4.17	Elemental quantitative data analysis represents TEOS-FAS-GO coated on the glass microslide	86
4.18	TGA-DTG data for TEOS sol at different TEOS concentrations	90
4.19	TGA-DTG data for TEOS-FAS at different FAS concentrations	92
4.20	TGA-DTG data for TEOS-FAS-SiO ₂ at different SiO ₂ concentrations	96
4.21	TGA-DTG data for TEOS-FAS-GO at different GO concentrations	97



LIST OF FIGURES

Figure		Page
1.1	The water contact angle (θ) – the angle that is taken from the angle occurred between the plane of a surface and the tangent from which the water droplet makes contact with the surface.	1
1.2	Scanning electron microscope image of <i>Nelumbo nucifera</i> leaf distinguishing high rough surface. A scale bar shown is 50 μm . An inset shows the original image of the leaf (Neinhuis & Barthlott, 1997).	2
1.3	SEM image of water striders leg. Spindle-like structures emanating off the leg contain nanosize grooved structure, contributed to dual-scale roughness to the leg. A secreted wax acts to repel water. (Scale bar – left = 20 μm and right = 200 nm)(Yan et al., 2011)	2
2.1	Schematic diagram presenting the 3-phase contact line of a water droplet on a solid surface as suggested by Young's mode.	8
2.2	The wetting characteristics of a water droplet distinguished by a) Young's mode; b) Wenzel's mode c) Cassie-Baxter's mode and d) Marmur mode	9
2.3	Young equation describes the contact of three phase namely solid-liquid, solid-vapor and liquid-vapor	11
2.4	(a) Schematic of Work of cohesion, (b) schematic of work of adhesion	12
2.5	A basic of Zisman plot in which $\cos\theta$ is plotted versus surface tension of liquid	15
3.1	Scheme showing (a) the hydrolysis of TEOS upon adding with water and (b) condensation step. (where R is an alkyl chain. For TEOS, R = $-\text{CH}_2\text{CH}_3$)	29
3.2	Scheme showing the reaction mechanism occurred between TEOS and FAS	30
3.3	Scheme showing the reaction mechanism between TEOS-FAS and Silica.	31

3.4	Scheme showing the reaction mechanism between TEOS-FAS and GO	32
3.5	Schematic flow charts for the sol gel synthesis of hydrophobic coating and its derivatives.	34
3.6	Schematic formulation of hydrophobic coating by spraying deposition technique using (a) silica and (b) GO by sol-gel method	35
3.7	a) Schematic of basic setup of sessile drop method b) Sessile drop that is fitted with contour	38
3.8	Fitting of contact angle of a droplet by Young Laplace equation on top of the coated glass microslide	39
3.9	Example of an image from surface profiler measurement $Z(M)-Z(R) = 10.170 \mu\text{m}$ (bold) represents thickness of the coated sample	40
4.1	Binding energy for TEOS sol and TEOS-FAS sol	42
4.2	Binding energy for TEOS-FAS-Silica-1 and Silica-5	42
4.3	Binding energy for TEOS-FAS-GO-1 and TEOS-FAS-GO-5	43
4.4	Deconvolution of Si2p peak of (a) TEOS, (b) TEOS-FAS, (c) Silica-1, (d) Silica-5, (e) GO-1, and (f) GO-5 coatings	45-47
4.5	Deconvolution of O1s peak of (a) TEOS, (b) TEOS-FAS, (c) Silica-1, (d) Silica-5, (e) GO-1, and (f) GO-5 coatings	49-52
4.6	Deconvolution of C1s peak of (a) TEOS-FAS, (b) Silica-1, (c) Silica-5, (d) GO-1, and (e) GO-5 coatings	53-55
4.7	Deconvolution of F1s peak of (a) TEOS-FAS, (b) Silica-1, (c) Silica-5, (d) GO-1, and (e) GO-5 coatings	57-59
4.8	FTIR spectrum obtained of bare glass	61
4.9	FTIR spectra of TEOS at different concentration	62
4.10	FTIR spectra of TEOS at different concentration at $4000-1500 \text{ cm}^{-1}$	63
4.11	FTIR spectra of TEOS at different concentration at $1300-600 \text{ cm}^{-1}$	63

4.12	FTIR spectra of TEOS-FAS at different concentration	65
4.13	FTIR spectra of TEOS-FAS at different concentration at 4000-1200 cm ⁻¹	66
4.14	FTIR spectra of TEOS-FAS at different concentration at 1375-600 cm ⁻¹	66
4.15	FTIR spectra of TEOS-FAS-SiO ₂ at different concentration	68
4.16	FTIR spectra of TEOS-FAS-SiO ₂ at different concentration at 4000-2400 cm ⁻¹	69
4.17	FTIR spectra of TEOS-FAS-SiO ₂ at different concentration at 1900-1300 cm ⁻¹	69
4.18	FTIR spectra of TEOS-FAS-SiO ₂ at different concentration at 1350-700 cm ⁻¹	70
4.19	FTIR spectra of TEOS-FAS-GO at different concentration	72
4.20	FTIR spectra of TEOS-FAS-GO at different concentration at 4000-1450 cm ⁻¹	73
4.21	FTIR spectra of TEOS-FAS-GO at different concentration at 1300-600 cm ⁻¹	73
4.22	UV-Visible spectra for TEOS sol coatings	75
4.23	UV-Visible spectra for TEOS-FAS sol coatings	76
4.24	UV-Visible spectra for TEOS-FAS-SiO ₂ sol coatings	77
4.25	UV-Visible spectra for TEOS-FAS-GO sol coatings	79
4.26	FESEM micrograph of (a) TEOS and (b) TEOS-FAS (mag. 10kx)	80
4.27	EDX spectrum for (a) TEOS and (b) TEOS-FAS coated on the glass microslide	81
4.28	FESEM micrograph of TEOS-FAS-SiO ₂ : (a) mag. 2 kx and (b) 10 kx	83
4.29	EDX spectrum for TEOS-FAS-Silica coated on the glass microslide	83

4.30	FESEM micrograph of TEOS-FAS-GO: (a) mag. 2 kx and (b) 10 kx	85
4.31	EDX spectrum for TEOS-FAS-Silica coated on the glass microslide	85
4.32	2D and 3D AFM images for (a) TEOS sol and (b) TEOS-FAS	87
4.33	2D and 3D AFM images for (a) Silica-1 and (b) Silica-5	88
4.34	2D and 3D AFM images for (a) GO-1 and (b) GO-5	89
4.35	(a) DTG and (b) TGA curve of TEOS sol gel film at different concentrations	91
4.36	(a) DTG and (b) TGA curve of TEOS-FAS sol gel film at different concentrations	93
4.37	(a) DTG and (b) TGA curve of TEOS-FAS-SiO ₂ sol gel film at different concentrations	95
4.38	(a) DTG and (b) TGA curve of TEOS-FAS-GO sol gel film at different concentrations	98
4.39	(a) Water contact angle and (b) surface free energy for TEOS sol at different TEOS concentrations	100-101
4.40	(a) Water contact angle and (b) surface free energy for TEOS sol at different FAS concentrations	102-103
4.41	Fluoroalkyl silane structure used in the study	103
4.42	(a) Water contact angle and (b) surface free energy for TEOS-FAS sol at different silica concentrations	105-106
4.43	(a) Water contact angle and (b) surface free energy for TEOS-FAS sol at different graphene oxide concentrations	107-108
4.44	Water contact angle after peeling test for (a) TEOS, (b) TEOS-FAS (c) TEOS-FAS-Silica and (d) TEOS-FAS-GO	109-111

LIST OF ABBREVIATIONS

AFM	Atomic Force Microscopy
APTEOS	Aminopropyltriethoxysilane
ASTM	American Standard Testing Method
ATR	Attenuated Total Reflectance
CNT	Carbon nanotube
Co ₃ O ₄	Cobalt oxide
CVD	Chemical vapor deposition
DSA	Drop shape analysis
DTG	Derivative Thermogravimetry
EDX	Energy Dispersive X-Ray
EQS	Equation of State
Eu	Europium complex
f_A	Surface fraction of air
FAS	Fluoroalkylsilane
FESEM	Field Emission Scanning Electron Microscopy
FG	Fluorographene
f_S	Surface fraction of solid
FTIR	Fourier Transform Infra-Red
G	Graphene
GO	Graphene oxide
H ₂ O	Water
HCl	Hydrochloric acid
HDMS	Hexamethyldisilazane
HDMSO	Hexamethyldisiloxane
HDPE	High density polyethylene
ITO	Indium tin oxide
L_A	Liquid air interface
LBL	Layer by layer assembly
L_S	Liquid solid interface
L_V	Liquid vapor interface
MMT	Montmorillonite clay
MTMS	Methyltrimethoxysilane
N.A.	Not Available
PDMS	Polydimethylsiloxane
PDVB	Polydivinylbenzene
PEG	Polyethylene glycol
PET	Polyethylene terephthalate
PFTS	Perfluorooctyl trichlorosilane
PMMA	Polymethyl methacrylate
pph	Parts per hundred
PQ	Performance qualification
PS	Polystyrene
PU	Polyurethane
r	Surface roughness factor
r_{ms}	Root mean square
R_a	Roughness average
R_p	Maximum profile peak height

R_q	rms Roughness
R_t	Maximum height of the profile
R_v	Maximum profile valley depth
SEM	Scanning Electron Microscopy
SFE	Surface free energy
SiO_2	Silica
T	Transmittance
T_{max}	Maximum temperature
Ta_2O_5	Tantalum pentoxide
TEOS	Tetraorthosilicate
TGA	Thermogravimetric Analysis
TiO_2	Titania
UV	Ultraviolet
UV-Visible	Ultraviolet-Visible Spectroscopy
W_A	Work of adhesion
WCA	Water Contact Angle
XPS	X-Ray Photoelectron Spectroscopy
Z_{max}	Highest peak
Z_{min}	Lowest valley
$Z(M)$	Maximum peak
$Z(R)$	Average profile
ZnO	Zinc oxide
θ_c	Contact angle in Marmur mode
θ_c and θ_Y	Contact angle in Young's mode
θ_T	Threshold contact angle between Wenzel and Cassie & Baxter mode
γ_{AB}	Interfacial tension for vapor for A and B phase
γ_{AV}	Surface tension for vapor for A phase
γ_{BV}	Surface tension for vapor for B phase
γ_{LV}	Surface energy of liquid against vapor
γ_{SL}	Surface energy of surface against liquid
γ_{SV}	Surface energy of surface against vapor
θ	Contact angle
θ_A	Contact angle of air
θ_{CB}	Contact angle in Cassie & Baxter mode
θ_S	Contact angle of solid
θ_W	Contact angle on a rough surface
γ_{SV}^h	Surface tension of hydrogen
γ_{SV}^{ab}	Surface tension of dispersion acid base
γ_{SV}^d	Surface tension of dispersion
γ_{SV}^o	Surface tension of all interaction
γ_{SV}^p	Surface tension of polar

CHAPTER 1

INTRODUCTION

1.1 Overview of Transparent Water Repellent Coating

Water repellent coating refers to a coating that contains surface water contact angle (θ), (Figure 1.1) (WCA) greater than 90° . If the WCA obtained is less than 90° , the coating is addressed as hydrophilic. And if it is higher than that, it is called hydrophobic and if it is greater than 150° , the coating is called as water superrepellent or superhydrophobic (Das et al., 2018).

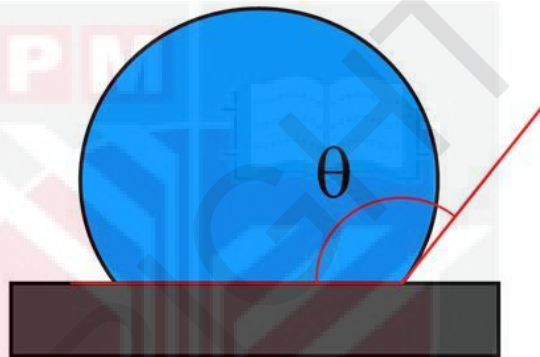


Figure 1.1: The water contact angle (θ) – the angle that is taken from the angle occurred between the plane of a surface and the tangent from which the water droplet in contact with the surface.

Water repellent surface can be observed in nature. It varies between hydrophobic and superhydrophobic. The Lotus effect (a name given after the Lotus plant, *Nelumbo nucifera*) is the name that describes self-cleaning phenomenon of some leaf surfaces (Figure 1.2). When the leaf distinguishes high water repellency, water shall form close-spherical droplets that reel across the surface instead of sliding. The reeling phenomenon collects foreign body dirt and debris and thereby clean the surface naturally. The greater self-cleaning phenomena can be observed for rougher surface. The plant leaves which possess waxy coatings but poor rough microstructure is not so efficient at self-cleaning. Contrary with the leaves that possess both characteristics namely waxy coatings and rough surface, the self-cleaning is more efficient (Neinhuis & Barthlott, 1997).

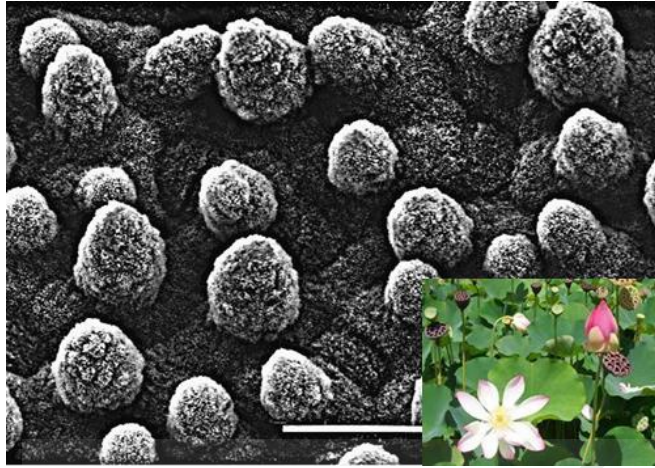


Figure 1.2: SEM image of *Nelumbo nucifera* leaf distinguishing high roughness surface. A scale bar shown is 50 μm . An inset shows the original image of the leaf (Neinhuis & Barthlott, 1997).

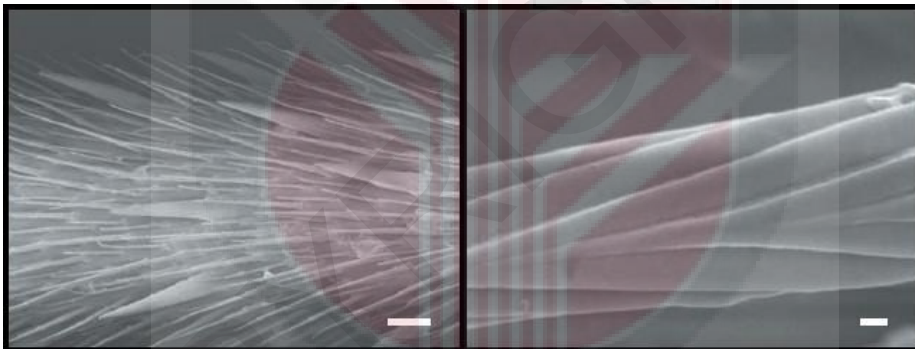


Figure 1.3: SEM image of water striders leg. Spindle-like structures emanating off the leg contain nanosize grooved structure, contributed to dual-scale roughness to the leg. A secreted wax acts to repel water. (Scale bar – left = 20 μm and right = 200 nm)(Yan et al., 2011)

High water repellency in nature can also be observed in animal for example water strider legs. Its legs contain greatly defined microstructure as well as layered with secreted wax (Figure 1.3). Some insect wings also possess water repellent properties attributed to surface microstructure and its composition. These include dragon fly, butterfly wings, as well as penguin skin.

These surface properties and their usefulness in nature as described above have provided inspiration to the scientific communities to design artificial water repellent surface that has great potentials in self-cleaning coatings, anti-microbial, automotive windows, and anti-corrosion.

As of 2015, the hydrophobic coating in the world market size was USD 1.34 billion and it is expected that there will be witnessed a significant growth in the future owing to its high demand in automotive, aerospace and construction industry (<https://www.grandviewresearch.com/industry-analysis/hydrophobic-coating-market>). In addition, the innovations to employ the nanoparticles in hydrophobic coatings that provide the high surface area and improved performance has opened new avenues for the industry growth over the expected period.

1.2 Problem Statement

Nowadays, to produce durable and transparent water repellent coating is a great challenge. There are several inorganic nanoparticles and transparent polymers that can be employed to synthesize transparent water repellent coating but the water repellency of this artificial coating always suffer degradation due to robust outdoor environment that lessens the water repellency characteristic. In natural lotus leaves, the continuous water repellency is attributed to the continuous metabolism of their surface wax layer and thus maintain the water repellency during their life time.

The scientists and researchers very often do not report the degree of transparency of the water repellent coatings. The main reason which can be presumed is the water repellent coating is normally optically translucent. It is in our knowledge that water repellency is contributed by high surface roughness and hydrophobic chemical composition. The limited report obtained for the transparency of water repellent coating is because both characteristics are in competition with each other. By enhancing surface roughness, it shall increase the surface water repellency but simultaneously enhance the scattered light falls on a surface which is addressed as Mie scattering. This scattering occurs when the diameter of the scattering particles is near to the incident light wavelength and thus is identified as the main factor in reducing the optical transparency of water repellent surface (Mie, 1908; Yu et al., 2015).

There are several methods to synthesize transparent water repellent coating include plasma processing, electrospinning, chemical and physical deposition but those methods require high voltage of electricity, high content of chemical residues and environmental unfriendly (Celia et al., 2013). Sol gel technique is found the best method to overcome these problems (Gu et al., 2017; Das et al., 2018). In addition, there are several approaches to control optical transparency of water repellent coating include chemical vapor deposition and solution immersion method. However, spray coating which was used in this study appears as the most practical, low cost, scalable and well adapted technique to coat small to large substrate with various geometries. The transparent characteristic can be controlled by spray-coating process whereas water repellency can be regulated by adjusting the loading amount of long chain fluoroalkylsilane as well as the amount GO and Silica. (Yang et al., 2009; Mahadik et al., 2016)

1.3 Scope of Study

The aim of this study is to synthesize transparent water repellent coating comprises of tetraorthosilicate, TEOS that will act as precursor, fluoroalkylsilane; FAS which works as hydrophobic agent and graphene oxide, GO and silica respectively that work as nanofiller that is possible in enhancing the roughness of the coating surface. Silica is one of the conventional nanofillers that are usually applied in hydrophobic study. However, the durability of silica incorporated water repellent coating becomes a concern among scientist. Thus, the employment of GO in this study is to investigate its potential in this field as well as to look at the durability of GO incorporated water repellent coating. Sol gel method is used because of ease to synthesis, cheap and feasible (Mahadik et al., 2017; Tadanaga et al., 1997) while the spraying technique is proposed to deposit the coating formulation onto the surface of glass microslide substrate because as compared to other techniques, such as dipping, brushing and spin coating, it promises adaptability and controlled thickness (Yang et al., 2009).

1.4 Objectives of the Study

The general aim of this study is to prepare water repellent coatings either in hydrophobic or superhydrophobic range by mean of sol gel technique and to study the effect of fluorination of fluoroalkylsilane with GO and silica nanofillers respectively on the morphology and topography of the sample, water contact angle, transmittance degree, vibrational assignment of chemical molecules and surface chemistry. Thus, the objectives of the study are concluded as follows:

- i. to develop a transparent water repellent formulation by sol gel method and subsequently produce the water repellent coating deposited on glass microslides by spraying technique.
- ii. to identify the vibrational assignment of chemical molecules and surface chemistry of the water repellent coating at different concentrations of TEOS, FAS, GO and silica nanofillers respectively for determining the functional groups and elemental composition involved in the sol gel reaction of the coating formulations.
- iii. to characterize the optical transparency, surface morphology and topography of the water repellent coating at different concentrations of TEOS, FAS, GO and silica nanofillers respectively for determining the surface roughness.
- iv. to investigate the thermal and hydrophobic properties of the water repellent coating at different concentration of TEOS, FAS, GO and silica nanofillers respectively.

1.5 Significances of the Study

The research shall determine the potential of graphene derivative namely graphene oxide in the synthesis of water repellent coating. The characterizations that were carried out are compared with silica incorporated water repellent coating especially on the parameter of the water contact angle and the durability of the measured water repellency. Silica, being a nanofiller that enhance the surface roughness has been studied extensively in superhydrophobic coating area. The price of this material is also affordable which is good for commercialization.

However, it also contains hindrance which include issues on its durability and dispersibility (Shen et al., 2010) . This can be overcome by using graphene oxide in which graphene, a derivative from carbon materials is excellent in thermal, mechanical and environmental stability. Graphene alone is not suitable because it is very inert and difficult to be dissolved in common solvents (Yang et al., 2017). The incorporation of graphene oxide can also give additional characteristic such as the coating is more conductive which is good in optoelectronic device.

In addition, the utilization of graphene oxide as a nanofillers in the fabrication of superhydrophobic thin sol gel film in comparison with other materials such as silica (Kavale et al., 2011; Mahadik et al., 2016; Sun et al., 2017) and fluorinated polymers (Ma and Hill, 2006; Lin et al., 2010; Mundo, et al., 2008) is quite limited because the research on superhydrophobic graphene and its derivative are in its early stage. Besides that, how to manipulate the full use of superhydrophobic graphene and its derivatives. Despite water repellent ability, graphene possesses several other merits include mechanical strength, high surface area, flexibility and optical transparency (Potts et al., 2011; Artilles et al., 2011), It can be anticipated that the synergy between outstanding characteristics of graphene and its derivatives with water repellency can provide to novel applications in the field of optoelectronics, electronic devices and anti-microbial (Wang et al., 2015). An exciting future for superhydrophobic graphene shall be witnessed and it is all due to the contribution of multidisciplinary scientists and engineers in the designing of such surfaces.

1.6 Thesis Outlines

In **Chapter 1**, the overview of water repellent coating and problem statement in relation to the study is discussed. In addition, the scope of the research and the objectives are also reported. The significance of study is mentioned at the end of the chapter.

In **Chapter 2**, the first phase of this chapter reviews the basic theory in water repellency and the models reported by earlier scientists. Then the past and present methods in producing synthetic water repellent coating from different materials are reviewed thoroughly in the next phase of the chapter.

In **Chapter 3**, the methodology in synthesizing water repellent coating by sol gel technique is discussed. The first part consists of the preparation of (TEOS) sol, followed by tetraorthosilicate-fluoroalkylsilane (TEOS-FAS) and finally tetraorthosilicate-fluoroalkylsilane-silica formulation and tetraorthosilicate-fluoroalkylsilane-graphene oxide formulation.

In **Chapter 4**, the results and discussion pertaining to the samples prepared are reported. The water contact angle or WCA, UV-Visible, FESEM, AFM, FTIR and XPS were reported in order to characterize the hydrophobicity, transmittance degree, surface morphology and topography, vibrational assignment of molecules and surface elemental analysis of water repellent coatings.

In **Chapter 5**, a conclusion from the finding is presented. The way forward as a continuity of the present work is also being proposed.

REFERENCES

- Abbas, R., Elkhoshkhany, N., Hefnawy, A., Ebrahim, S., & Rahal, A. (2017). High stability performance of superhydrophobic modified fluorinated graphene films on copper alloy substrates. *Advances in Materials Science and Engineering*, 2017, 1–8.
- Abbasi, M., & Hashemi, B. (2014). Fabrication and characterization of bioactive glass-ceramic using soda lime silica waste glass. *Materials Science & Engineering C*, 37, 399–404.
- Adeoye, A. E., Ajenifuja, E., Taleatu, B. A., & Fasasi, A. Y. (2015). Rutherford backscattering spectrometry analysis and structural properties of $Zn_xPb_{1-x}S$ thin films deposited by chemical spray pyrolysis. *Journal of Materials*, 2015, 1–8.
- Alam, A. U., Howlader, M. M. R., & Deen, M. J. (2013). Oxygen plasma and humidity dependent surface analysis of silicon, silicon dioxide and glass for direct wafer bonding. *ECS Journal of Solid State Science and Technology*, 2(12), 515–523.
- Ariffin, E. Y., Ahmad, A., Mohamad, D., & Mohamed, M. (2011). Effect of molecular weight on the properties of liquid epoxidised natural rubber acrylate (LENRA)/silica hybrid composites. *Sains Malaysiana*, 40(7), 743–748.
- Artiles, M. S., Rout, C. S., & Fisher, T. S. (2011). Graphene-based hybrid materials and devices for biosensing. *Advanced Drug Delivery Reviews*, 63(14–15), 1352–1360.
- Asgari, M., Abouelmagd, A., & Sundararaj, U. (2017). Silane functionalization of sodium montmorillonite nanoclay and its effect on rheological and mechanical properties of HDPE/clay nanocomposites. *Applied Clay Science*, 146, 439–448.
- Barankin, M. D., Williams, T. S., Li, E. G., & Hicks, R. F. (2010). Properties of fluorinated silica glass deposited at low temperature by atmospheric plasma-enhanced chemical vapor deposition. *Thin Solid Films*, 519(4), 1307–1313.
- Bareiro, O., & Santos, L. A. (2014). Tetraethylorthosilicate (TEOS) applied in the surface modification of hydroxyapatite to develop polydimethylsiloxane/hydroxyapatite composites. *Colloids and Surfaces B: Biointerfaces*, 115, 400–405.
- Barkhudarov, P. M., Shah, P. B., Watkins, E. B., Doshi, D. A., Brinker, C. J., & Majewski, J. (2008). Corrosion inhibition using superhydrophobic films. *Corrosion Science*, 50(3), 897–902.

- Barnat-Hunek, D., & Smarzewski, P. (2015). Surface free energy of hydrophobic coatings of hybrid-fiber-reinforced high-performance concrete. *Materiali in Tehnologije*, 49(6), 895–902.
- Barr, T. L. (1983). An XPS study of Si as it occurs in adsorbents, catalysts, and thin films. *Applications of Surface Science*, 15(1-4), 1-35.
- Barshilia, H. C., John, S., & Mahajan, V. (2012). Nanometric multi-scale rough, transparent and anti-reflective ZnO superhydrophobic coatings on high temperature solar absorber surfaces. *Solar Energy Materials and Solar Cells*, 107, 219–224.
- Basu, B. J., Hariprakash, V., Aruna, S. T., Lakshmi, R. V., Manasa, J., & Shruthi, B. S. (2010). Effect of microstructure and surface roughness on the wettability of superhydrophobic Sol-gel nanocomposite coatings. *Journal of Sol-Gel Science and Technology*, 56(3), 278–286.
- Bayer, I. S., Steele, A., Martorana, P. J., & Loth, E. (2010). Fabrication of superhydrophobic polyurethane/organoclay nano-structured composites from cyclomethicone-in-water emulsions. *Applied Surface Science*, 257(3), 823–826.
- Bebensee, F., Voigts, F., & Maus-Friedrichs, W. (2008). The adsorption of oxygen and water on Ca and CaO films studied with MIES, UPS and XPS. *Surface Science*, 602(9), 1622-1630.
- Bravo, J., Zhai, L., Wu, Z., Cohen, R. E., & Rubner, M. F. (2007). Transparent superhydrophobic films based on silica nanoparticles. *Langmuir*, 23(13), 7293–7298.
- Booshehri, A. Y., Goh, S. C. K., Hong, J., Jiang, R., & Xu, R. (2014). Effect of depositing silver nanoparticles on BiVO₄ in enhancing visible light photocatalytic inactivation of bacteria in water. *Journal of Materials Chemistry A*, 2(17), 6209-6217.
- Cai, Z., Lin, J., & Hong, X. (2018). Transparent superhydrophobic hollow films (TSHFs) with superior thermal stability and moisture resistance. *RSC Advances*, 8(1), 491–498.
- Carr, N., Goodwin, M. J., Harrison, K. J., & Lewis, K. L. (1993). The design and fabrication of optical filters using organic materials. *Thin Solid Films*, 230(1), 59–64.
- Cassie, A. B. D., & Baxter, S. (1944). Wettability of porous surfaces. *Transactions of the Faraday Society*, 40, 546-551.
- Celia, E., Darmanin, T., Taffin de Givenchy, E., Amigoni, S., & Guittard, F. (2013a). Recent advances in designing superhydrophobic surfaces. *Journal of Colloid and Interface Science*, 402, 1–18.

- Chen, H., Huang, S., & Perng, T. (2012). Preparation and characterization of molecularly homogeneous silica-titania film by sol-gel process with different synthetic strategies. *Applied Materials and Interfaces* 4(10), 5188-5195.
- Chinh, V. U. D. U. C., Broggi, A., Palma, L. D. I., Scarsella, M., Speranza, G., & Vilardi, G. (2017). XPS spectra analysis of Ti^{2+} , Ti^{3+} ions and dye photodegradation evaluation of titania-silica mixed oxide nanoparticles. *Journal of Electronic Materials*, 47(4), 2215-2224.
- Cui, X., Ding, R., Wang, M., Wang, C., Zhang, J., Wang, J., Dong, W. & Xu, Y. (2017). A hydrophobic and abrasion-resistant MgF₂ coating with an ultralow refractive index for double-layer broadband antireflective coatings. *Journal of Materials Chemistry C*, 5(12), 3088–3096.
- Das, S., Kumar, S., Samal, S. K., Mohanty, S., & Nayak, S. K. (2018). A Review on Superhydrophobic Polymer Nanocoatings: Recent Development and Applications. *Industrial and Engineering Chemistry Research*, 57(8), 2727–2745.
- De Moraes, A. C. M. D., Andrade, P. F., De Faria, A. F., Simões, M. B., Salomão, F. C. C. S., Barros, E. B., Goncalves, M. D. C. & Alves, O. L. (2015). Fabrication of transparent and ultraviolet shielding composite films based on graphene oxide and cellulose acetate. *Carbohydrate Polymers*, 123, 217–227.
- Deshmukh, S. C., & Aydil, E. S. (1995). Investigation of SiO₂ plasma enhanced chemical vapor deposition through tetraethoxysilane using attenuated total reflection Fourier transform infrared spectroscopy. *Journal of Vacuum Science & Technology A: Vacuum, Surfaces, and Films*, 13(5), 2355–2367.
- Drdacky, M., Lesák, J., Rescic, S., Slížková, Z., Tiano, P., & Valach, J. (2012). Standardization of peeling tests for assessing the cohesion and consolidation characteristics of historic stone surfaces. *Materials and Structures*, 45(4), 505-520.
- Du, J., Luo, X., Fu, Z., Xu, C., Ren, X., Gao, W., & Li, Y. (2015). Improving the hydrophobicity of nylon fabric by consecutive treatment with poly(acrylic acid), tetraethylorthosilicate, and octadecylamine. *Journal of Applied Polymer Science*, 132(34), 1–7.
- Eluyemi, M. S., Eleruja, M. A., Adedeji, A. V., Olofinjana, B., Fasakin, O., Akinwunmi, O. O., Ajayi, E. O. B. (2016). Synthesis and Characterization of Graphene Oxide and Reduced Graphene Oxide Thin Films Deposited by Spray Pyrolysis Method. *Graphene*, 05(03), 143–154.
- Erbil, H. Y. (2014). The debate on the dependence of apparent contact angles on drop contact area or three-phase contact line: A review. *Surface Science Reports*, 69(4), 325–365.

- Fan, P., Chen, J., Yang, J., Chen, F., & Zhong, M. (2017). GO@CuSilicate nano-needle arrays hierarchical structure: a new route to prepare high optical transparent, excellent self-cleaning and anticorrosion superhydrophobic surface. *Journal of Nanoparticle Research*, 19(2).
- Feng, L., Li, S., Li, Y., Li, H., Zhang, L., Zhai, J., Zhu, D. (2002). Superhydrophobic surfaces: From natural to artificial. *Advanced Materials*, 14(24), 1857–1860.
- Fowkes, F. M. (1964). Attractive forces at interfaces. *Industrial & Engineering Chemistry*, 56(12), 40–52.
- Funano, S. I., Tanaka, N., & Tanaka, Y. (2016). Vapor-based micro/nano-partitioning of fluoro-functional group immobilization for long-term stable cell patterning. *RSC Advances*, 6(98), 96306–96313.
- Ganjoo, S., Azimirad, R., Akhavan, O., & Moshfegh, A. Z. (2008). Persistent superhydrophilicity of sol-gel derived nanoporous silica thin films. *Journal of Physics D: Applied Physics*, 42(2), 025302.
- Gao, L., & He, J. (2013). Surface hydrophobic co-modification of hollow silica nanoparticles toward large-area transparent superhydrophobic coatings. *Journal of Colloid and Interface Science*, 396, 152–159.
- Ghosh, P., Satou, S., Nakamori, H., Noda, T., Daisuke, I., & Tanemura, M. (2012). Facile one-step fabrication of highly transparent and flexible superhydrophobic substrate by room-temperature ion irradiation method. *Physica Status Solidi - Rapid Research Letters*, 6(11), 430–432.
- Gu, L., Wang, Y., Xu, C., Zhang, F., Wu, Z., Zhang, X., Shi, Z. & Peng, C. (2017). Construction of superhydrophobic surfaces by sol-gel techniques. In 2017 *IEEE International Conference on Manipulation, Manufacturing and Measurement on the Nanoscale (3M-NANO)* (pp. 156-160).
- Gui-Long, X., Changyun, D., Yun, L., Pi-hui, P., Jian, H., & Zhuoru, Y. (2011). Preparation and characterization of raspberry-like SiO₂ particles by the sol-gel method. *Nanomaterials and Nanotechnology*, 1(2), 79–83.
- Gustus, R., Gruber, W., Wegewitz, L., Geckle, U., Prang, R., & Kübel, C. (2014). Decomposition of amorphous Si₂C by thermal annealing, *Thin Solid Films*, 552, 232–240.
- Haeri, S. Z., Ramezanzadeh, B., & Asghari, M. (2017). A novel fabrication of a high performance SiO₂-graphene oxide (GO) nanohybrids: Characterization of thermal properties of epoxy nanocomposites filled with SiO₂-GO nanohybrids. *Journal of Colloid and Interface Science*, 493, 111–122.
- Han, J. T., Kim, S. Y., Woo, J. S., & Lee, G.-W. (2008). Transparent, Conductive, and Superhydrophobic Films from Stabilized Carbon Nanotube/Silane Sol Mixture Solution. *Advanced Materials*, 20(19), 3724–3727.

- Harun, M. H., Talib, Z. A., Ghazali, N., Salleh, N., Mohamed, M., Alias, M. S., & Ibrahim, N. A. *Transparent hydrophobic coating by sol gel method*. Paper presented at Seminar R&D Agensi Nuklear Malaysia, Oct 2016.
- Harun, M. H., Talib, Z. A., Ibrahim, N. A., Chyi, J. L. Y., Salleh, N. G. N., Alias, M. S. & Othman, N. (2018). Characterization of transparent hydrophobic coating with silica and graphene oxide fillers by sol-gel method. *International Journal of Nanoelectronics and Materials*, 11(3), 283–292.
- He, Z., Ma, M., Lan, X., Chen, F., Wang, K., Deng, H. & Fu, Q. (2011). Fabrication of a transparent superamphiphobic coating with improved stability. *Soft Matter*, 7(14), 6435–6443.
- Hench, L. L., & West, J. K. (1990). The sol-gel process. *Chemical Reviews*, 90(1), 33-72.
- Her, E. K., Ko, T. J., Shin, B., Roh, H., Dai, W., Seong, W. K., Kim, H. Y., Lee, K. R., Oh, K. H. & Moon, M. W. (2013). Superhydrophobic transparent surface of nanostructured poly(methyl methacrylate) enhanced by a hydrolysis reaction. *Plasma Processes and Polymers*, 10(5), 481–488.
- Holtzinger, C., Niparte, B., Wächter, S., Berthomé, G., Riassetto, D., & Langlet, M. (2013). Superhydrophobic TiO₂ coatings formed through a non-fluorinated wet chemistry route. *Surface Science*, 617, 141–148.
- Hozumi, A., Ushiyama, K., Sugimura, H., & Takai, O. (1999). Fluoroalkylsilane Monolayers Formed by Chemical Vapor Surface Modification on Hydroxylated Oxide Surfaces, 14(18), 7600–7604.
- Hwangbo, S., Heo, J., Lin, X., Choi, M., & Hong, J. (2016). Transparent superwetting nanofilms with enhanced durability at model physiological condition. *Scientific reports*, 6, 19178.
- Ibrahem, S., & Ibrahem, H. (2014). Synthesis and Study the Effect of H₂O/TEOS ratio of the Silica xerogel by Sol-Gel method. *International Archive of Applied Sciences and Technology*, 5, 1-5.
- Imamora, M., Umar, A., Chin, C., & Rozidawati, Y. (2016). Effect of thermal reduction temperature on the optical and electrical properties of multilayer graphene. *Journal of Materials Science: Materials in Electronics*, 2–5.
- Irzh, A., Ghindes, L., & Gedanken, A. (2011). Rapid deposition of transparent super-hydrophobic layers on various surfaces using microwave plasma. *Applied Materials & Interfaces* 3, 4566–4572.
- Jeevajothi, K., Crossiya, D., & Subasri, R. (2012). Non-fluorinated , room temperature curable hydrophobic coatings by sol – gel process. *Ceramics International*, 38(4), 2971–2976.

- Ji, H., Chen, G., Hu, J., Wang, M., Min, C., & Zhao, Y. (2013). Biomimetic Superhydrophobic Surfaces. *Journal of Dispersion Science and Technology*, 34(1), 1–21.
- Jiang, C., Zhang, Y., Wang, Q., & Wang, T. (2013). Superhydrophobic polyurethane and silica nanoparticles coating with high transparency and fluorescence. *Journal of Applied Polymer Science*, 129(5), 2959–2965. <https://doi.org/10.1002/app.39024>.
- Kavale, M. S., Mahadik, D. B., Parale, V. G., Wagh, P. B., Gupta, S. C., Rao, A. V., & Barshilia, H. C. (2011). Applied Surface Science Optically transparent , superhydrophobic methyltrimethoxysilane based silica coatings without silylating reagent. *Applied Surface Science*, 258(1), 158–162.
- Kerker, M. (1969) *The Scattering Of Light*. New York: Academic Press.
- Kim, D. H., & Lee, D. H. (2019). Effect of irradiation on the surface morphology of nanostructured superhydrophobic surfaces fabricated by ion beam irradiation. *Applied Surface Science*, 477, 154-158.
- Kim, M., Kim, K., Lee, N. Y., Shin, K., & Kim, Y. S. (2007). A simple fabrication route to a highly transparent super-hydrophobic surface with a poly(dimethylsiloxane) coated flexible mold. *Chemical Communications*, (22), 2237–2239.
- Kim, D. J., Hwang, H. Y., & Nam, S. Y. (2013). Characterization of sulfonated poly (arylene ethersulfone)(SPAES)/silica-phosphate sol-gel composite membrane: Effects of the sol-gel composition. *Macromolecular Research*, 21(11), 1194-1200.
- Kuru, D. (2019). The effect of piranha and silane modifications on boron nitride nanosheets (bnns) thin film formation. *Cumhuriyet Science Journal* 40 (2) 424–432.
- Lai, Y., Tang, Y., Gong, J., Gong, D., Chi, L., Lin, C., & Chen, Z. (2012). Transparent superhydrophobic/superhydrophilic TiO₂-based coatings for self-cleaning and anti-fogging. *Journal of Materials Chemistry*, 22(15), 7420–7426.
- Lakshmi, R. V, Bera, P., Anandan, C., & Basu, B. J. (2014). Effect of the size of silica nanoparticles on wettability and surface chemistry of sol–gel superhydrophobic and oleophobic nanocomposite coatings. *Applied Surface Science*, 320, 780–786.
- Lakshmi, R. V, Bharathidasan, T., Bera, P., & Basu, B. J. (2012). Surface & Coatings Technology Fabrication of superhydrophobic and oleophobic sol-gel nanocomposite coating. *Surface & Coatings Technology*, 206(19–20), 3888–3894.

- Latthe, S. S., Sutar, R. S., Bhosale, A. K., Nagappan, S., Ha, C. S., Sadasivuni, K. K., Liu, S. & Xing, R. (2019). Recent developments in air-trapped superhydrophobic and liquid-infused slippery surfaces for anti-icing application. *Progress in Organic Coatings*, 137(2019), 1-17.
- Lee, Y. (2007). Syntheses and properties of fluorinated carbon materials, *Journal of Fluorine Chemistry*, 128, 392–403.
- Levkin, P. A., Svec, F., & Fréchet, J. M. J. (2009). Porous polymer coatings: A versatile approach to superhydrophobic surfaces. *Advanced Functional Materials*, 19(12), 1993–1998.
- Li, D., & Neumann, A. W. (1992). Contact angles on hydrophobic solid surfaces and their interpretation. *Journal of Colloid And Interface Science*, 148(1), 190–200.
- Li, Jian, Wan, H., Ye, Y., Zhou, H., & Chen, J. (2012). One-step process to fabrication of transparent superhydrophobic SiO₂ paper. *Applied Surface Science*, 261, 470–472.
- Li, Jindi, Xu, J., Wang, B., & Guo, Z. (2013). Transparent and Superhydrophobic Co₃O₄ Microfiber Films. *Chemistry Letters*, 43(1), 100–101.
- Li, L., Gu, W., Liu, J., Yan, S., & Xu, Z. P. (2014). Amine-functionalized SiO₂ nanodot-coated layered double hydroxide nanocomposites for enhanced gene delivery. *Nano Research*, 8(2) 882–694.
- Li, R., Chen, C., Li, J., Xu, L., Xiao, G., & Yan, D. (2014). A facile approach to superhydrophobic and superoleophilic graphene/polymer aerogels. *Journal of Materials Chemistry A*, 2(9), 3057–3064.
- Li, W., & Amirfazli, A. (2005). A thermodynamic approach for determining the contact angle hysteresis for superhydrophobic surfaces. *Journal of colloid and interface science*, 292(1), 195-201.
- Lin, Y. H., Liao, K. H., Huang, C. K., Chou, N. K., Wang, S. S., Chu, S. H., & Hsieh, K. H. (2010). Superhydrophobic films of UV-curable fluorinated epoxy acrylate resins. *Polymer international*, 59(9), 1205-1211.
- Lin, Y., Ehlert, G. J., Bukowsky, C., & Sodano, H. A. (2011). Superhydrophobic functionalized graphene aerogels. *ACS Applied Materials and Interfaces*, 3(7), 2200–2203.
- Liravi, M., Pakzad, H., Moosavi, A., & Nouri-Borujerdi, A. (2020). A comprehensive review on recent advances in superhydrophobic surfaces and their applications for drag reduction. *Progress in Organic Coatings*, 140, 105537.

- Liu, M., Zhang, Y., Wu, C., Xiong, S., & Zhou, C. (2012). Chitosan/halloysite nanotubes bionanocomposites: structure, mechanical properties and biocompatibility. *International Journal of Biological Macromolecules*, 51(4), 556-575
- Liu, J., Kim, G. H., Xue, Y., Kim, J. Y., Baek, J. B., Durstock, M., & Dai, L. (2014). Graphene oxide nanoribbon as hole extraction layer to enhance efficiency and stability of polymer solar cells. *Advanced Materials*, 26(5), 786–790.
- Liu, S., Liu, X., Latthe, S. S., Gao, L., An, S., & Yoon, S. S. (2015). Applied Surface Science Self-cleaning transparent superhydrophobic coatings through simple sol – gel processing of fluoroalkylsilane. *Applied Surface Science*, 351, 897–903.
- Ma, W. S., Li, J., Deng, B. J., & Zhao, X. S. (2013). Preparation and characterization of long-chain alkyl silane-functionalized graphene film. *Journal of Materials Science*, 48(1), 156–161.
- Macias-Montero, M., Borrás, A., Romero-Gomez, P., Cotrino, J., Frutos, F., & Gonzalez-Elipé, A. R. (2014). Plasma deposition of superhydrophobic Ag@TiO₂ Core@shell nanorods on processable substrates. *Plasma Processes and Polymers*, 11(2), 164–174.
- Mahadik, S. A., Kavale, M. S., Mukherjee, S. K., & Rao, A. V. (2010). Applied Surface Science Transparent Superhydrophobic silica coatings on glass by sol-gel method. *Applied Surface Science*, 257(2), 333–339.
- Mahadik, S. A., Pedraza, F., & Vhatkar, R. S. (2016). Silica based superhydrophobic coating for long-term industrial and domestic applications. *Journal of Alloys and Compounds*, 663, 487–493.
- Manakasettharn, S., Hsu, T.-H., Myhre, G., Pau, S., Taylor, J. A., & Krupenkin, T. (2012). Transparent and superhydrophobic Ta₂O₅ nanostructured thin films. *Optical Materials Express*, 2(2), 214.
- Marmur, A. (2003). Wetting on hydrophobic rough surfaces: To be heterogeneous or not to be? *Langmuir*, 19(2), 8343.
- Martin, S., & Bhushan, B. (2017). Transparent, wear-resistant, superhydrophobic and superoleophobic poly(dimethylsiloxane) (PDMS) surfaces. *Journal of Colloid and Interface Science*, 488, 118–126.
- Mathkar, A., Narayanan, T. N., Alemany, L. B., Cox, P., Nguyen, P., Gao, G., Ajayan, P. M. (2013). Synthesis of FGO and its amphiphobic properties. *Particle and Particle Systems Characterization*, 30(3), 266–272.
- Miankafshe, M. A., Bashir, T. & Persson N. K. (2019). The role and importance of surface modification of polyester fabrics by chitosan and hexadecylpyridinium chloride for the electrical and electro-thermal performance of graphene-modified smart textiles. *New Journal of Chemistry*. 43, 6643–6658.

- Mie, G. 1908. Beiträge zur Optik trüber Medien, speziell kolloidaler Metallösungen. *Annalen der Physik (Translation)* 330(3): 377–445.
- Miloskovska, E., Friedrichs, C., Hristova-Bogaerds, D., Persenair, O., van Duin, M., Hansen, M. R., & de With, G. (2015). Chemical Mapping of Silica Prepared via Sol–Gel Reaction in Rubber Nanocomposites. *Macromolecules*, 48(4), 1093-1103.
- Moulder, J. F., Stickle, W. F., Sobol, P. E., & Bomben, K. D. (1992). *Handbook of X-ray Photoelectron Spectroscopy*, edited by J. Chastain Perkin-Elmer Corporation.
- Mundo, R. D., Palumbo, F., & D'Agostino, R. (2008). Nanotexturing of polystyrene surface in fluorocarbon plasmas: from sticky to slippery superhydrophobicity. *Langmuir*, 24(9), 5044–5051.
- Munief, W., Lu, X., Teucke, T., Wilhelm, J., Britz, A., Hempel, F., Lanche, R., Schwartz, M, Law, J. K. Y., Grandthyll, S., Müller, F., Neurohr, J. U., Jacobs, K., Schmitt, M., Pachauri, V. Hempelmann, R. & Ingebrandt, S. (2019). Reduced graphene oxide biosensor platform for the detection of NT-proBNP biomarker in its clinical range. *Biosensors and Bioelectronics*, 126, 136–142.
- Nahum, T., Dodiuk, H., Kenig, S., Panwar, A., Barry, C., & Mead, J. (2017). The effect of composition and thermodynamics on the surface morphology of durable superhydrophobic polymer coatings. *Nanotechnology, Science and Applications*, 10, 53–68.
- Nakagawa, T., & Soga, M. (1999). A new method for fabricating water repellent silica films having high heat-resistance using the sol gel method, *Journal of Non-Crystalline Solids*, 260, 167–174.
- Neinhuis, C. & Barthlott, W. (1997). Characterization and Distribution of Water-repellent, Self-cleaning Plant Surfaces. *Annals of Botany*, 79(6), 667–677.
- Niemeyer, W. D. (2015). Proceeding of SPIE: SEM/EDS analysis for problem solving in the food industry. In *Scanning Microscopies* (Vol. 9636, p. 96360G). International Society for Optics and Photonics.
- Nishino, T., Masashi, M., Katsuhiko, N., Motonori, M., & Yasukiyo, U. (1999). The lowest surface free energy based on -CF₃ alignment. *Langmuir*, 15(7), 4321–4323.
- Nosonovsky, M., & Bhushan, B. (2007). Hierarchical roughness optimization for biomimetic superhydrophobic surfaces. *Ultramicroscopy*, 107(10–11), 969–979.
- Nosonovsky, M., & Bhushan, B. (2008). Patterned nonadhesive surfaces: superhydrophobicity and wetting. *Langmuir: The ACS Journal of Surfaces and Colloids*, 24, 1525–1533.

- Olejniczak, Z., Łęczka, M., Cholewa-Kowalska, K., Wojtach, K., Rokita, M., & Mozgawa, W. (2005). ^{29}Si MAS NMR and FTIR study of inorganic–organic hybrid gels. *Journal of Molecular Structure*, *744*, 465–471.
- Owens, D. K., & Wendt, R. C. (1969). Estimation of the surface free energy of polymers. *Journal of Applied Polymer Science*, *13*(8), 1741–1747.
- Park, H. K., Yoon, S. W., Chung, W. W., Min, B. K., & Do, Y. R. (2013). Fabrication and characterization of large-scale multifunctional transparent ITO nanorod films. *Journal of Materials Chemistry A*, *1*(19), 5860–5867.
- Peng, M., Liao, Z., Qi, J., & Zhou, Z. (2010). Nonaligned Carbon nanotubes partially embedded in polymer matrixes: a novel route to superhydrophobic conductive surfaces. *Langmuir*, *26*(16), 13572–13578.
- Picolo, N., Moraes, V. T. D., Lebrão, G. W., & Lebrão, S. M. G. (2019). Sol-gel processed Superhydrophobic Plastic Surfaces Modified with Perfluorooctyltriethoxysilane (POTS). *Materials Research*, *22*, 1-10.
- Post, P., Wurlitzer, L., Maus-friedrichs, W., & Weber, A. P. (2018). Characterization and applications of nanoparticles modified in-flight with silica or silica-organic coatings, *Nanomaterials*, *8*, 1–19.
- Potts, J. R., Dreyer, D. R., Bielawski, C. W., & Ruoff, R. S. (2011). Graphene-based polymer nanocomposites. *Polymer*, *52*(1), 5–25.
- Privett, B. J., Youn, J., Hong, S. A., Lee, J., Han, J., Shin, J. H., & Schoenfish, M. H. (2011). Antibacterial fluorinated silica colloid superhydrophobic surfaces. *Langmuir*, *27*(15), 9597–9601.
- Qi, D., Lu, N., Xu, H., Yang, B., Huang, C., Xu, M., Gao, L., Wang, Z. & Chi, L., (2009). Simple approach to wafer-scale self-cleaning antireflective silicon surfaces. *Langmuir*, *25*(14), 7769–7772.
- Ramezanzadeh, B., Ahmadi, A., & Mahdavian, M. (2016). Enhancement of the corrosion protection performance and cathodic delamination resistance of epoxy coating through treatment of steel substrate by a novel nanometric sol-gel based silane composite film filled with functionalized GO nanosheets. *Corrosion Science*, *109*, 182–205.
- Rivero, P. J., Maeztu, J. D., Berlanga, C., Miguel, A., Palacio, J. F., & Rodriguez, R. (2018). Hydrophobic and corrosion behavior of sol-gel hybrid coatings based on the combination of TiO_2 NPs and fluorinated chains for aluminum alloys protection. *Metals*, *8*(12) 1–18.
- Romero, R., A., Tamburini, S., Taveri, G., Toušek, J., Dlouhy, I., & Bernardo, E. (2018). Extension of the ‘inorganic gel casting’ process to the manufacturing of boro-alumino-silicate glass foams. *Materials*, *11*(12), 2545–2557.

- Rubio, F., Rubio, J., & Oteo, J. L. (1998). A FT-IR study of the hydrolysis of tetraethylorthosilicate (TEOS). *Spectroscopy Letters*, 31(1), 199–219.
- Rulison, C. (1999). Measure surface energy: A tutorial designed to provide basic understanding of the concept of solid surface energy. *Kruss USA*, 40.
- Saharudin, K. A., Karim, M. A., & Sreekantan, S. (2019). Preparation of a Polydimethylsiloxane (PDMS)/graphene-based superhydrophobic coating. *Materials Today: Proceedings*, 17, 752–760.
- Santucci, S., Di Nardo, S., Lozzi, L., Passacantando, M., & Picozzi, P. (1995). XPS analysis on SiO₂ sol-gel thin films. *Journal of Electron Spectroscopy and Related Phenomena*, 76, 623–628.
- Schuster, J. M., Schvezov, C. E., & Rosenberger, M. R. (2015). analysis of the results of surface free energy measurement of Ti6Al4V by different methods. *Procedia Materials Science*, 8, 732–741.
- Shang, Q., & Zhou, Y. (2016). Fabrication of transparent superhydrophobic porous silica coating for self-cleaning and anti-fogging. *Ceramics International*, 42(7), 8706–8712.
- Shen, J., Li, N., Shi, M., Hu, Y., & Ye, M. (2010). Covalent synthesis of organophilic chemically functionalized graphene sheets. *Journal of Colloid and Interface Science*, 348(2), 377–383.
- Si, Y., & Guo, Z. (2015a). Superhydrophobic nanocoatings: from materials to fabrications and to applications. *Nanoscale*, 7(14), 5922–5946.
- Smitha, S., Shajesh, P., Mukundan, P., & Warriar, K. G. K. (2008). Sol-gel synthesis of biocompatible silica-chitosan hybrids and hydrophobic coatings. *Journal of Materials Research*, 23(8), 2053–2060.
- Steele, A., Bayer, I., Moran, S., Cannon, A., King, W. P., & Loth, E. (2010). Conformal ZnO nanocomposite coatings on micro-patterned surfaces for superhydrophobicity. *Thin Solid Films*, 518(19), 5426–5431.
- Sun, Z., Liu, B., Huang, S., Wu, J., & Zhang, Q. (2017). Facile fabrication of superhydrophobic coating based on polysiloxane emulsion. *Progress in Organic Coatings*, 102, 131–137.
- Tadanaga, K., Katata, N., & Minami, T. (1997). Super-waterrepellent Al₂O₃ coating films with high transparency. *Journal of the American Ceramic Society*, 80(4), 1040–1042.
- Tapasa, K., Pantulap, U., Petchareanmongkol, B., & Kaewdang, W. (2019). Effect of SiO₂ contents in TEOS-SiO₂-OTES hybrid coating on glass. *Key Engineering Materials*, 798 KEM, 128–133.

- Tarwal, N. L., & Patil, P. S. (2010). Superhydrophobic and transparent ZnO thin films synthesized by spray pyrolysis technique. *Applied Surface Science*, 256(24), 7451–7456.
- Teshima, K., Sugimura, H., Inoue, Y., Takai, O., & Takano, A. (2005). Transparent ultra water-repellent poly(ethylene terephthalate) substrates fabricated by oxygen plasma treatment and subsequent hydrophobic coating. *Applied Surface Science*, 244(1–4), 619–622.
- Topuz, B., Şimşek, D., & Çiftçioğlu, M. (2014). Preparation of monodisperse silica spheres and determination of their densification behaviour. *Ceramics International*, 41(1), 43–52.
- Torres-Carrasco, M., Palomo, A., & Puertas, F. (2014). Sodium silicate solutions from dissolution of glass wastes. Statistical analysis. *Materiales de Construcción*, 64(314), 1–12.
- Tricoli, A., Righettoni, M., & Pratsinis, S. E. (2009). Anti-fogging nanofibrous SiO_2 and nanostructured SiO_2 - TiO_2 films made by rapid flame deposition and in situ annealing. *Langmuir*, 25(21), 12578–12584.
- Tu, K., Kong, L., Wang, X., & Liu, J. (2016). Semitransparent, durable superhydrophobic polydimethylsiloxane/ SiO_2 nanocomposite coatings on varnished wood. *Holzforschung*, 70(11), 1039–1045.
- van Oss, C. J., Chaudhury, M. K., & Good, R. J. (1988). Interfacial Lifshitz—van der Waals and Polar Interactions in Macroscopic Systems. *Chemical Reviews*, 88(6), 927–941.
- Vidal, K., Gómez, E., Goitandia, A. M., Angulo-Ibáñez, A., & Aranzabe, E. (2019). The synthesis of a superhydrophobic and thermal stable silica coating via sol-gel process. *Coatings*, 9(10) 1–13.
- Wang, C. F., Tzeng, F. S., Chen, H. G., & Chang, C. J. (2012). Ultraviolet-durable superhydrophobic zinc oxide-coated mesh films for surface and underwater-oil capture and transportation. *Langmuir*, 28(26), 10015–10019.
- Wang, J. N., Zhang, Y. L., Liu, Y., Zheng, W., Lee, L. P., & Sun, H. B. (2015). Recent developments in superhydrophobic graphene and graphene-related materials: from preparation to potential applications. *Nanoscale*, 7(16), 7101–7114.
- Wang, C., Yang, H., Chen, F., Peng, L., Gao, H. fang, & Zhao, L. P. (2018). Influences of VTMS/ SiO_2 ratios on the contact angle and morphology of modified super-hydrophobic silicon dioxide material by vinyl trimethoxy silane. *Results in Physics*, 10, 891–902.

- Wang, F., Wang, X., Xie, A., Shen, Y., Duan, W., Zhang, Y., & Li, J. (2012). A simple method for preparation of transparent hydrophobic silica-based coatings on different substrates. *Applied Physics A: Materials Science and Processing*, 106(1), 229–235.
- Wang, H., Fang, J., Cheng, T., Ding, J., Qu, L., & Dai, L. (2008). One-step coating of fluoro-containing silica nanoparticles for universal generation of surface superhydrophobicity. *Chemical Communications*, (7) 877–879.
- Wenzel, R. N. (1936). Resistance of solid surfaces to wetting by water. *Industrial and Engineering Chemistry*, 28(8), 988–994.
- Wisniak, J. (2010). Daniel Berthelot . Part I . *Educación Química*, 21(2), 155–162.
- Wu, S., & Brzozowski, K. J. (1971). Surface free energy and polarity of organic pigments. *Journal of Colloid And Interface Science*, 37(4), 686–690.
- Xia, B., Yan, L., Li, Y., Zhang, S., He, M., Li, H., Jiang, B. (2018). Preparation of silica coatings with continuously adjustable refractive indices and wettability. *RSC Advances*, 8, 6091–6098.
- Xiong, J., Jin, Y., Shentu, B., & Weng, Z. (2013). Preparation and fluorine enrichment behavior of fluorinated polyester. *Journal of Coatings Technology and Research*, 10(5), 621–629.
- Xu, Q. F., Liu, Y., Lin, F. J., Mondal, B., & Lyons, A. M. (2013). Superhydrophobic TiO₂-polymer nanocomposite surface with UV-induced reversible wettability and self-cleaning properties. *ACS Applied Materials and Interfaces*, 5(18), 8915–8924.
- Yabu, H., & Shimomura, M. (2005). Single-step fabrication of transparent superhydrophobic porous polymer films, *Chemistry of Materials*, 11(4), 5231–5234.
- Yan, Y. Y., Gao, N., & Barthlott, W. (2011). Mimicking natural superhydrophobic surfaces and grasping the wetting process : A review on recent progress in preparing superhydrophobic surfaces. *Advances in Colloid and Interface Science*, 169(2), 80–105.
- Yang, G. H., Bao, D. D., Liu, H., Zhang, D. Q., Wang, N., & Li, H. Tao. (2017). Functionalization of Graphene and Applications of the Derivatives. *Journal of Inorganic and Organometallic Polymers and Materials*, 27(5), 1129–1141.
- Yang, J., Zhang, Z., Men, X., & Xu, X. (2009). Fabrication of stable, transparent and superhydrophobic nanocomposite films with polystyrene functionalized carbon nanotubes. *Applied Surface Science*, 255(22), 9244–9247.

- Yang, Z., Wang, L., Sun, W., Li, S., Zhu, T., Liu, W., & Liu, G. (2017). Superhydrophobic epoxy coating modified by fluorographene used for anti-corrosion and self-cleaning. *Applied Surface Science*, 401, 146–155.
- Yao, W., Bae, K., Yung, M., & Cho, Y. (2017). Transparent, conductive, and superhydrophobic nanocomposite coatings on polymer substrate. *Journal of Colloid And Interface Science*, 506, 429–436.
- Yilbas, B. S., Ibrahim, A., Ali, H., Khaled, M., & Laoui, T. (2018). Applied surface science hydrophobic and optical characteristics of graphene and graphene oxide films transferred onto functionalized silica particles deposited glass surface. *Applied Surface Science*, 442, 213–223.
- Yoon, Y., Lee, D. W., & Lee, J. B. (2013). Fabrication of optically transparent PDMS artificial lotus leaf film using underexposed and underbaked photoresist mold. *Journal of Microelectromechanical Systems*, 22(5), 1073–1080.
- Young, T. (1804). An essay to the cohesion of fluids. *Philosophical Transaction of the Royal Society of London*, (95) 65–87.
- Zarzosa, G. O., Araujo-Andrade, C., Compean-Jasso, M. E., Martinez, J. R., & Ruiz, F. (2002). Cobalt oxide/silica xerogels powders: X-ray diffraction, infrared and visible absorption studies. *Journal of Sol-Gel Science and Technology*, 24(1), 23-29.
- Zhang, X., Kono, H., Liu, Z., Nishimoto, S., Tryk, D. A., Murakami, Sakai, H., Abe, M., & Fujishima, A. (2007). A transparent and photo-patternable superhydrophobic film. *Chemical Communications*, (46), 4949–4951.
- Zhang, F., Shi, Z., Jiang, Y., Xu, C., Wu, Z., Wang, Y., & Peng, C. (2017). Fabrication of transparent superhydrophobic glass with fibered-silica network. *Applied Surface Science*, 407, 526–531.
- Zhang, Y. L., Wang, J. N., He, Y., He, Y., Xu, B. Bin, Wei, S., & Xiao, F. S. (2011). Solvothermal synthesis of nanoporous polymer chalk for painting superhydrophobic surfaces. *Langmuir*, 27(20), 12585–12590.
- Zhang, Y., Li, J., Huang, F., Li, S., Shen, Y., Xie, A., Wang, F. (2013). Controlled fabrication of transparent and superhydrophobic coating on a glass matrix via a green method. *Applied Physics A: Materials Science and Processing*, 110(2), 397–401.
- Zhao, Q., Liu, Y., & Abel, E. W. (2004). Effect of temperature on the surface free energy of amorphous carbon films. *Journal of Colloid and Interface Science*, 280(1), 174–183.
- Zisman, W. A. (1964). Relation of the Equilibrium Contact Angle to Liquid and Solid Constitution, *Advances in Chemistry Series. Advances in Chemistry*. 43: 1–51.